Proc. Natl. Acad. Sci. USA
Vol. 89, pp. 8581–8585, September 1992
Neurobiology

Localization of the protein kinase C phosphorylation/calmodulin-binding substrate RC3 in dendritic spines of neostriatal neurons

(third messenger/forebrain-enriched protein/postsynaptic sites/synaptogenesis/neuronal plasticity)

JOSEPH B. WATSON*, J. GREGOR SUTCLIFFE†, AND ROBIN S. FISHER‡

*Department of Psychiatry and Biobehavioral Sciences, Mental Retardation Research Center and Brain Research Institute, UCLA School of Medicine, Los Angeles, CA 90024; †Department of Molecular Biology, The Scripps Research Institute, La Jolla, CA 92037; and ‡Departments of Psychiatry and Biobehavioral Sciences/Anatomy and Cell Biology, Mental Retardation Research Center and Brain Research Institute, UCLA School of Medicine, Los Angeles, CA 90024

Communicated by Charles H. Sawyer, April 6, 1992 (received for review January 22, 1992)

ABSTRACT **The rodent protein RC3 is expressed mainly by forebrain neurons during postnatal development and maturity. RC3 and its bovine homolog neurogranin/B-50 immunoreactive C-kinase substrate (BICKS) contain overlapping sites for protein kinase C phosphorylation and calmodulin binding that resemble those of the presynaptic 43-kDa growth-associated protein (GAP-43). However, morphological evidence suggests that RC3 has a postsynaptic localization. To test this hypothesis, we used two polyclonal antisera against synthetic peptides corresponding to nonoverlapping sequences within RC3 and compared cellular distributions of their binding in neostriatum of adult rats by immunohistochemistry, Golgi impregnation/gold toning, and correlative light/electron microscopy. Somatic and punctate patterns of RC3 immunoreactivity were observed. Somatic RC3 was found in cyto- and nucleoplasmic compartments of all neuronal phenotypes (medium spiny, medium aspiny, and large aspiny cells). Punctate RC3 was found mostly in dendritic spines. In contrast to the 43-kDa growth-associated protein, RC3 was seen infrequently in axons. We conclude that RC3 accumulates postsynaptically in dendritic spines of neostriatal neurons. We propose that RC3 acts as a "third messenger" substrate of protein kinase C-mediated molecular cascades during synaptic development and remodeling.**

RC3 is a 78-amino acid protein that was first identified in rodent forebrain by screening a cDNA library with a neocortex-minus-cerebellum subtracted cDNA probe (1). RC3 is found principally in neostriatum, neocortex, and hippocampus. The bovine protein kinase C (PKC) substrate neurogranin and calmodulin-binding protein B-50 immunoreactive C-kinase substrate (BICKS) are structural homologs (75/78 amino acids) of RC3 (2, 3). The cellular localization and function of these proteins are largely unknown. Part of RC3 resembles overlapping PKC phosphorylation and calmodulin-binding sites of the 43-kDa growth-associated protein (GAP-43) (1–9). However, RC3 and GAP-43 have distinct properties. GAP-43 is located along the entire neuraxis and accumulates mostly in presynaptic profiles of forebrain axons during early synaptic formation or after injury (9, 10). RC3 is located mostly in the telencephalon and is believed to accumulate in neuronal cell bodies and dendrites during development and maturity (1, 11).

Previous hybridization and immunohistochemical studies show that RC3 mRNA and RC3 protein are expressed in the same characteristic kinds of neuronal cell bodies in neostriatum, neocortex, and hippocampus (1, 11). However, a dendritic localization of RC3 protein is uncertain because of potential cross-reactivity between GAP-43 and RC3 antibodies. This problem is acute in forebrain regions with heterogeneous cell compositions. The relationship between RC3 and synaptic junctions is also uncertain because earlier studies are based on light microscopy, a morphological technique of inadequate precision to resolve subcellular sites of proteins. We now address these two issues with antisera that detect nonoverlapping domains of RC3. One antisera excludes the region of RC3/GAP-43 similarity. We used multiple labels (Nissl, Golgi, and immunohistochemical stains) and correlative light/electron microscopy (LM/EM) to determine RC3 cell phenotypes and ultrastructural sites among neostriatal neurons of adult rats.

METHODS

Polyclonal antibodies directed against synthetic peptides corresponding to two separate domains of RC3 were produced in rabbits as described (1, 12). RC3-1 antiserum was generated against a 27-amino acid peptide corresponding to an RC3 internal sequence (ILDIPLDDPGANAAAAKIQASFRGHMA) with part of the phosphorylation/calmodulin-binding domains shared with GAP-43 (see Fig. 1*A*). RC3-5 antiserum was generated against a 13-amino acid peptide corresponding to the RC3 C-terminal sequence (GARGGAGGGPSGD) devoid of GAP-43 sequence similarities (Fig. 1*A*).

Western blot analyses identified RC3 in unfixed protein extracts. Extraction and labeling procedures were detailed elsewhere (1, 13). Briefly, fresh tissue was dissected from adult rats killed by cervical dislocation. Experimental blots of regional brain extracts were incubated with either RC3-1 or RC3-5 antiserum and then with a goat anti-rabbit IgG alkaline phosphatase conjugate (13). Control blots were incubated in preimmune or antigen-presorbed sera (60 μg of peptide per ml).

Morphological analyses identified RC3 in fixed tissue sections (14). Ten adult rats were anesthetized with sodium pentobarbital [100 mg/kg (body weight)] and perfused with aldehyde fixative (1.33 mM paraformaldehyde/200 μM glutaraldehyde/0.1 M sodium phosphate). Coronal brain sections (100 μm thick, Vibratome) were treated to block endogenous oxidases and nonspecific IgG binding. Primary antisera were presorbed with acetone-extracted rat liver (20 mg/ml) to eliminate nonspecific labeling of cell nuclei. Experimental sections were incubated (18 h, room temperature, rotary agitation) in RC3-1 or RC3-5 antiserum. Empirically effective dilution ranges were 1:500–1:2000 (differential stain patterns of experimental and control sections). Control sections were incubated with comparable dilutions of primary

The publication costs of this article were defrayed in part by page charge payment. This article must therefore be hereby marked "*advertisement*" in accordance with 18 U.S.C. §1734 solely to indicate this fact.

Abbreviations: GAP-43, 43-kDa growth-associated protein; PKC, protein kinase C; LM and EM, light and electron microscopy, respectively.

preimmune serum, antigen-presorbed antiserum, nonimmune serum, or diluent. All sections were incubated with biotinylated goat anti-rabbit IgG and then with an avidin-peroxidase conjugate (ABC Vectastain Elite rabbit reagents) (15). Immunoreactivity was demonstrated histochemically with 3,3′-diaminobenzidine chromagen. Sections were then processed by three histological methods: (*i*) Nissl specimens (10 samples) were mounted, stained with cresyl violet (16), dehydrated, cleared, and cover-slipped for LM. (*ii*) Golgi specimens (3 samples) were osmicated, chromated, impregnated with silver chromate (17), transilluminated, gold toned, and deimpregnated (18) for LM. (*iii*) Correlative LM/EM specimens (3 samples) were dissected, osmicated, dehydrated, and embedded in Epon–Araldite (14). Adjacent semithin (toluidine blue counterstain) and thin sections (lead citrate poststain) were cut from immunoreactive faces of tissue blocks (14).

RESULTS

RC3 Western Blots. Both RC3-1 and RC3-5 antisera yielded similar and replicable patterns of RC3 labeling. All experimental blots exhibited the same single dense band of RC3 immunoreactivity in lanes of forebrain extracts (Fig. 1*B*). The mobility of the RC3 band was ≈15 kDa relative to markers and consistent with values from previous reports (1, 11). Control blots had no comparable labeling. At equivalent dilutions, RC3-1 antiserum produced more labeling than RC3-5 antiserum perhaps because of differences among antiserum titers, affinities, and/or antigenic epitopes.

The RC3 band was enriched in forebrain extracts and exhibited a typical regional distribution on all experimental blots. For both antisera, high amounts of RC3 were detected in neostriatum, cerebral cortex, and hippocampus (Fig. 1*B*). Low amounts were detected in olfactory bulb and hypothalamus with RC3-1 antiserum. RC3 was not detected in these regions with RC3-5 antiserum unless gels were overloaded with protein extracts. RC3 was not detected in retina, thalamus, cerebellum, pons, medulla, or spinal cord in any experimental blots.

Two other kinds of protein were also observed in experimental blots. RC3-1 antiserum detected a single faint band in several forebrain regions. The band had a molecular mass of 40–45 kDa consistent with the expected mobility of GAP-43. RC3-5 antiserum never detected this band. However, RC3-5 antiserum detected weak doublet bands of unknown identities with molecular masses of ≈30 kDa in retina and cerebellum, but not in forebrain regions.

Regionalization of RC3 in Tissue Sections. RC3-1 and RC3-5 antisera demonstrated specific, comparable, and replicable (10 of 10 samples) immunolabeling in experimental tissue sections. At comparable dilutions, preimmune serum, antigen-presorbed serum, nonimmune serum, and diluent produced no specific labeling in control tissue sections. RC3 immunoreactivity was enriched in forebrain and detected in nearly all forebrain gray matter. At the level of the decussation of the anterior commissure, high amounts of RC3 were distributed uniformly within neostriatum (+ nucleus accumbens) and low amounts were distributed in white matter tracts. In other sections, RC3 was detected in hippocampus, olfactory bulb, hypothalamus, and thalamus. RC3 was not detected in pons, cerebellum, medulla, and spinal cord. These data contrast with previous hybridization experiments reporting RC3 mRNA in pontine nuclei, deep cerebellar nuclei, and periaqueductal gray matter (1). The differences might reflect different sensitivities of method or relative rates of turnover for RC3 mRNA and RC3 protein.

Cytoarchitecture of RC3 Neurons. RC3 immunolabeling in neostriatum had two forms—cell bodies and puncta (Fig. 2 *A* and *B*). Similar results were obtained with RC3-1 and RC3-5 antisera. Previously, neurogranin-like immunoreactivity was located in cell bodies but not in puncta in rat neostriatum (11). RC3 antisera might have a greater affinity and/or specificity in rats than neurogranin antisera. As in Western blots of unfixed protein extracts, RC3-1 antiserum tended to produce a greater density of immunolabeling than RC3-5 antiserum.

RC3 immunoreactivity was contained in two kinds of neostriatal neurons as shown by cresyl violet and toluidine blue counterstains. In faces of sections (7–10 μm), nearly all neurons with perikaryal diameters >10 μm and nuclear diameters >5 μm were immunoreactive, and >95% had somatic diameters of 10–15 μm, nuclear diameters of 5–10 μm, pale basophilic cytoplasm, dispersed chromatin, and nucleoli corresponding to medium spiny and aspiny neostriatal neurons (Fig. 2 *A* and *B*) (19, 20). Their dendritic phenotypes were not differentiated by Nissl stains. A few (1–2%) had somatic diameters of 20–35 μm, nuclear diameters of 15–20 μm, dense basophilic cytoplasm, dispersed chromatin, and nucleoli corresponding to large aspiny neostriatal neurons (19, 20). Both kinds of neurons had flocculent

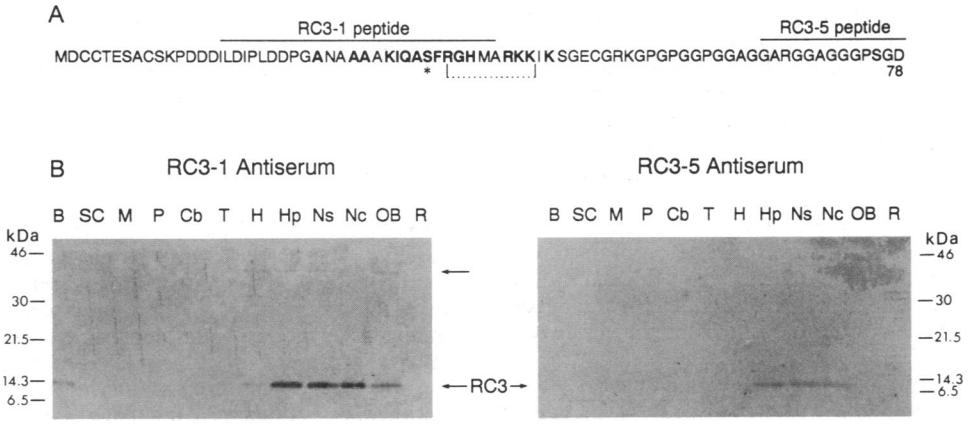

FIG. 1. RC3 amino acid sequence and Western blot analyses in adult rats. (*A*) RC3-1 and RC3-5 synthetic peptides used for antisera production are indicated (solid lines above corresponding amino acid sequences). Common sequences of RC3 and GAP-43 are indicated (boldface type). The PKC phosphorylation site is shown (asterisk) and the calmodulin-binding site is denoted (dotted line below sequence). (*B*) Western blots containing protein extracts (25–50 μg) from dissected brain regions were incubated with a 1:500 dilution of RC3-1 antiserum (on the left) or RC3-5 antiserum (on the right). Lanes: B, whole brain; SC, spinal cord; M, medulla; P, pons; Cb, cerebellum; T, thalamus; H, hypothalamus; Hp, hippocampus; Ns, neostriatum; Nc, neocortex; OB, olfactory bulb; R, retina. Based on protein standards (Amersham), an ≈15-kDa RC3 immunoreactive band was detected by both antisera (lower arrows). RC3-1 antiserum also detected a 40- to 45-kDa band (upper arrow) of possible cross-immunoreactivity with GAP-43.

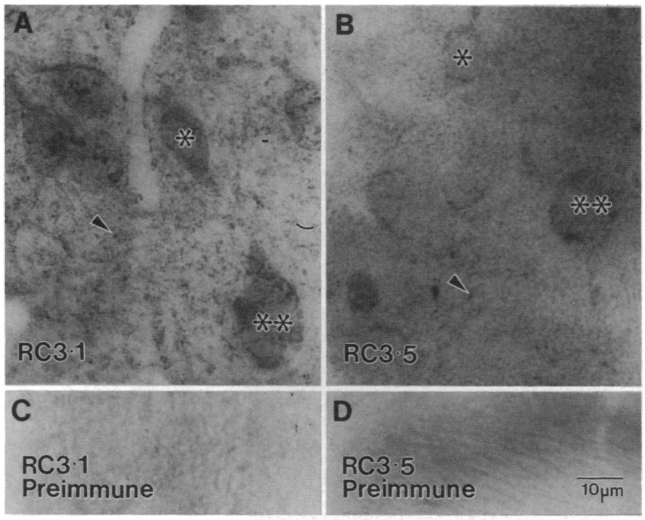

FIG. 2. Cellular distribution of RC3 immunoreactivity in neostriatum of adult rats. (*A*) RC3-1 antiserum labeled medium (single asterisk) and large (double asterisks) neurons plus many puncta scattered in the neuropil (arrowhead). (*B*) RC3-5 antiserum also labeled medium (single asterisk) and large (double asterisks) neurons plus many puncta scattered in the neuropil (arrowhead). No cells or punctae were labeled in control sections when RC3-1 antiserum was replaced by its preimmune serum (*C*) or RC3-5 antiserum was replaced by its preimmune serum (*D*).

and agranular immunoreactivity in perikaryal but not distal dendritic cytoplasm. Some cells also had immunoreactivity in nucleoplasm.

Dendritic phenotypes of RC3-containing neostriatal neurons were resolved in immunolabeled sections counterstained by Golgi impregnation/gold toning. Comparable results were obtained with RC3-1 and RC3-5 antisera. More than 500 gold-toned RC3 neostriatal neurons were examined in three tested cases. Doubly labeled neurons had red-brown

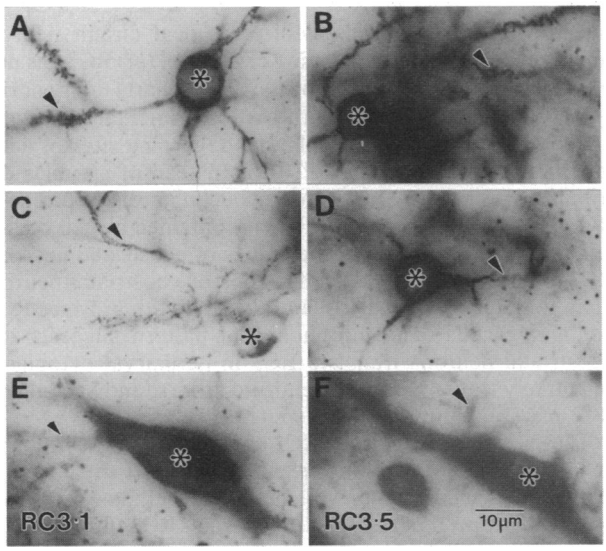

FIG. 3. Morphological phenotypes of RC3 neurons in the neostriatum of adult rats. RC3-immunolabeled cell bodies are denoted by asterisks and Golgi-gold toned dendrites originating from the same cells are shown by arrowheads. Chromatic differences of labels (red-brown immunoreactivity and translucent blue-gray Golgi/gold toned impregnation) were represented in photomicrographs by distinct gradients of label densities in cell bodies and proximal dendrites. RC3-1 antiserum labeled medium spiny (*A*), medium aspiny (*C*), and large aspiny neurons (*E*). RC3-5 antiserum labeled the same neuronal phenotypes (*B*, *D*, and *F*).

immunolabeling in the perikaryal cytoplasm that coincided with translucent blue-gray labeling of the perikaryal profile and dendritic arbor (Fig. 3). In control sections, RC3 and Golgi labeling were prevented singly and in combination to ensure accuracy of colocalization.

RC3 immunolabeling was represented proportionately among all structural phenotypes of neostriatal neurons. Medium spiny neurons most frequently showed the RC3 phenotype (>95% of doubly labeled cells; Fig. 3 *A* and *B*). They had somatic diameters of 10–15 μm and high spine densities (0.5–1.2 spines per μm of dendrite and branch orders of 3–7). Some of these neurons had somatic or proximal dendritic spines likely to reflect morphological variation within the phenotype (20). Medium aspiny neurons infrequently showed the RC3 phenotype (1–2% of doubly labeled cells; Fig. 3 *C* and *D*). They had somatic diameters of 10–15 μm, highly branched dendritic arbors, and low spine densities (0–0.01 spines per μm of dendrite and branch orders of 1–10). Large aspiny neurons also infrequently showed the RC3 phenotype (1–2% of doubly labeled cells; Fig. 3 *E* and *F*). They had somatic diameters of 20–35 μm and low spine densities (0–0.01 spines per μm of dendrite and branch orders of 1–7).

In neostriatum, RC3-containing puncta had few morphological features recognized by LM (Fig. 2 *A* and *B*). They had little Nissl counterstain and could not be discerned within darker Golgi counterstains of dendrites and unmyelinated axons (Fig. 3). RC3 puncta (diameters of 0.5–2.0 μm) resembled cross-sectional profiles of dendritic shafts, dendritic spines, and axons, but these specializations could not be distinguished by LM. Frequent RC3 puncta were dispersed uniformly throughout neostriatal gray matter in faces of tissue sections. RC3 punctae were rarely apposed to RC3 neurons and were scarcely found in perforant fascicles of the internal capsule.

Ultrastructure of RC3 Neurons. Peroxidase immunolabeling of RC3-containing cell bodies and puncta of the neostriatum was discerned in experimental semithin sections counterstained with toluidine blue. Osmicated and electron-dense immunolabeling of the same profiles was identified in adjacent thin sections examined by EM. Thin sections incubated with RC3-1 and RC3-5 antisera yielded similar ultrastructural patterns of immunolabeling. Control thin sections had no immunolabeling.

RC3-containing cells had the ultrastructural characteristics of neurons. They received sparse axosomatic afferents that established, for the most part, symmetrical synaptic junctions (21). Most RC3 neurons had profile diameters <10 μm, a thin rim of pale cytoplasm, sparse ribosomes, few perikaryal organelles, and simple endoplasmic reticulum (Fig. 4 *A* and *B*). They resembled medium spiny and aspiny neostriatal neurons (20). A few larger RC3 neurons had profile diameters >10 μm, a wide rim of dense cytoplasm, frequent ribosomes, a rich content of perikaryal organelles, and elaborate endoplasmic reticulum. They resembled large aspiny neostriatal neurons (20). In both kinds of neurons, dispersed cytoplasmic label was excluded from mitochondria and cisternae of endoplasmic reticulum (Fig. 4 *A* and *B*). Smaller RC3 neurons had spherical or indented nuclei and large RC3 neurons always had indented nuclei. RC3 was dispersed among nucleoplasmic euchromatin in both kinds of neurons.

In puncta, RC3 immunolabeling was observed principally in dendritic shafts and dendritic spines. Dendritic shafts and spine necks contained slight traces of RC3. In contrast, RC3-containing spine heads were the most frequent immunolabeled profiles and had the heaviest deposits of label in all cases (Fig. 4 *C* and *D*). RC3 spines often had a membranous spine apparatus in spine necks and established asymmetrical synaptic junctions along the spine head (21). RC3 immunolabeling often appeared to be most dense within the postsyn-

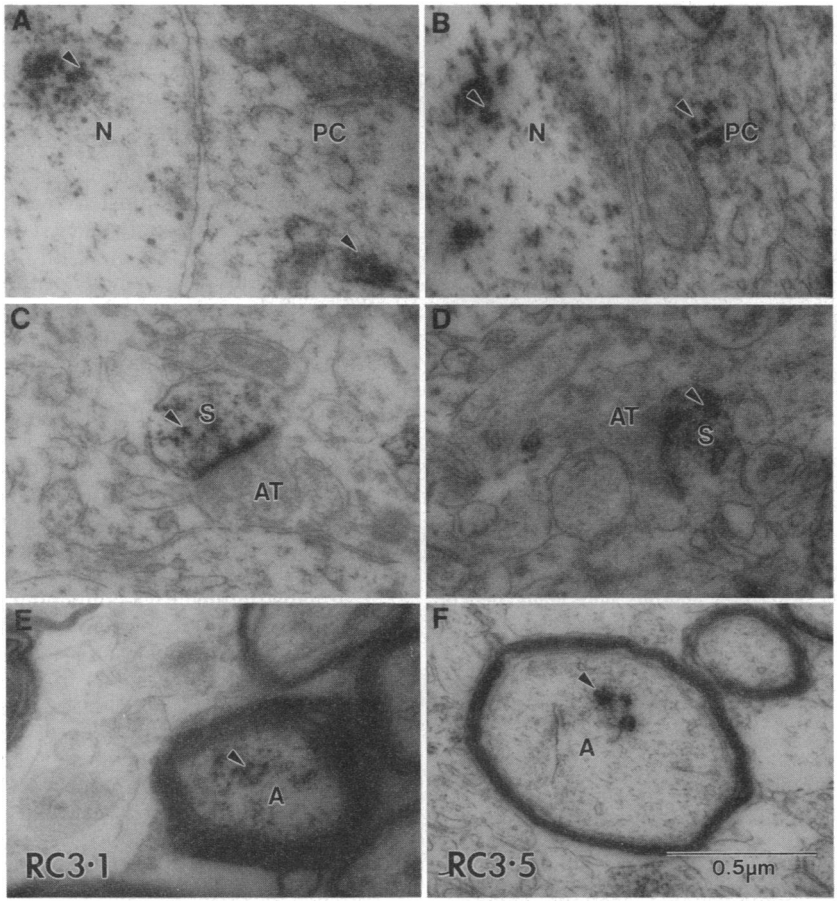

FIG. 4. Ultrastructural distribution of RC3 in the neostriatum of adult rats. Electron-dense immunolabeling is denoted by arrowheads. Within medium-sized neuronal cell bodies (all examples shown here), RC3-1 antiserum revealed immunolabeling in nucleoplasm (N) and perikaryal cytoplasm (PC) (*A*). RC3-5 antiserum yielded the same results (*B*). Within puncta of the neuropil, RC3-1 and RC3-5 antisera revealed immunolabeling mainly in dendritic spines (S) forming asymmetrical synaptic junctions with axonal terminals (AT) (*C* and *D*). RC3-1 and RC3-5 antisera also labeled a few myelinated axons (A) in fiber fascicles of the internal capsule (*E* and *F*).

aptic web of junctions (Fig. 4 *C* and *D*). Dense RC3 immunolabeling was not associated with postsynaptic webs of symmetrical or asymmetrical synaptic junctions along cell bodies and dendritic shafts. A few RC3-positive myelinated axons were found in fascicles of the internal capsule (Fig. 4 *E* and *F*). However, RC3 axons never penetrated the neuropil to establish synaptic junctions with neostriatal neurons.

DISCUSSION

We obtained three major observations concerning RC3 localization in neostriatum: (*i*) RC3 has now been detected reliably in unfixed brain protein extracts and fixed tissue sections by Western blot analysis and immunohistochemistry. RC3-1 and RC3-5 antisera yield similar results and are essentially monospecific. Results obtained with these well-characterized molecular probes are consistent with, but more detailed than, previous assessments of distributions of RC3 and neurogranin markers based on Northern blots, *in situ* hybridization, Western blots, and immunohistochemistry (1, 2, 11). (*ii*) RC3 has now been located precisely in different structural phenotypes of neostriatal neurons. RC3 detection in cell bodies and dendrites as defined by counterstains and ultrastructural methods refines regional and cellular distributions of RC3 delineated in previous experiments (1, 2). Neostriatal neurons have somatic and dendritic patterns of RC3 distribution that resemble cerebral cortex and hippocampus. Neostriatal RC3 accumulates in the receptive somatodendritic network of output plus local circuit neurons (medium spiny cells) and dedicated local circuit neurons (medium aspiny and large aspiny cells) (19). (*iii*) RC3 has now been found in deposits in postsynaptic parts of dendritic spines. This result agrees with our experimental hypothesis and confirms previous speculations regarding sites of accumulation and likely action of RC3. Instead of granular distributions expected from LM, subcellular distributions of RC3 are basically agranular. RC3 is contained by cell bodies, dendritic shafts, and dendritic spines of neostriatal neurons. RC3 is excluded from afferent axons of neostriatal neurons including local axonal collaterals originating from RC3-containing cells. The morphological pattern suggests that neostriatal neurons translate RC3 in perikaryal cytoplasm, selectively traffic RC3 into dendritic arbors, and accumulate RC3 mainly within dendritic spines.

The subcellular pattern of RC3 immunolabeling is probably an accurate and credible representation of principal sites of RC3 action within dendritic spines and perhaps within the postsynaptic web of neostriatal neurons. RC3 ultrastructure suggests an aldehyde-induced precipitation of a cytosolic protein along a sequestered route of synthesis and transport in cell bodies and dendrites (14). This interpretation agrees with preliminary Western blot experiments detecting RC3 mainly in cytosol, microsome, and synaptosome fractions of brain extracts (unpublished data). However, RC3 trafficking is not uniform in the forebrain. Myelinated RC3 axons in the internal capsule may depict a subset of corticofugal neurons that project to thalamus or midbrain and utilize RC3 in terminal axonal fields. There is no evidence of RC3 transport

in striatopetal axons (from cerebral cortex, thalamus, and midbrain), striatofugal axons (to pallidum and substantia nigra), or neostriatal intrinsic axons (19).

The nucleoplasmic pattern of RC3 immunolabeling is also credible. This is a frequent observation obtained from neurons with apparently intact membranes. Intercompartmental RC3 leakage is unlikely. Association of immunoreactivity with euchromatin suggests that RC3 may participate in regulation of transcription (15). This interpretation agrees with preliminary Western blot experiments detecting small amounts of RC3 in the nucleoplasm fraction of brain extracts (unpublished data). Nucleoplasmic and cytoplasmic localizations of RC3 are consistent with subcellular sites of protein kinases found in forebrain and cerebellar neurons (15).

The anatomy of RC3 points to the function and significance of RC3. (*i*) Restricted RC3 morphological patterns are important evidence for regional but not cellular selectivity within the PKC pathway of neurons in mammalian brain. (*ii*) RC3 is a forebrain-enriched postsynaptic protein mainly associated with dendritic spines. This is consistent with the coincidence of neostriatal spine genesis and RC3 mRNA expression during postnatal development (1, 22). RC3–spine relationships are also delineated by recent evidence that hypothyroidism depresses RC3 mRNA expression in neocortex and neostriatum, an effect reversed by hormone replacement during a critical postnatal period of spine genesis (23). (*iii*) RC3 expression by medium and large aspiny neurons seems to contradict this conclusion. Yet, these "aspiny" neurons actually generate transient spines in normal development and have sparse spines in normal maturity. It is reasonable to suspect that neostriatal neurons of diverse phenotypes maintain cytoplasmic pools of RC3 for utilization during spine formation and remodeling.

Postsynaptic RC3 fits the proposal that RC3 and GAP-43 may have comparable functions in anatomically but not temporally opposed parts of synapses in mammalian forebrain (2, 3, 11). We speculate that RC3 and GAP-43 act as "third messenger" substrates of PKC phosphorylation in respective post- and presynaptic transduction pathways (2, 24). In neostriatal neurons, RC3 lies in postsynaptic spines and GAP-43 lies in their presynaptic axon terminals (25). PKC phosphorylation of GAP-43 occurs during synaptic alterations of long-term potentiation (26, 27). These comparable RC3 and GAP-43 transduction pathways may promote coupling and coordination of axon–target interactions during synaptic formation and remodeling particularly in axospinous corticostriatal connections (19, 25). In these events, PKC phosphorylation and calmodulin binding are likely to have central post- and presynaptic roles mediated by conserved domains in RC3 and GAP-43 (2). Dissimilar domains of RC3 and GAP-43 may contribute to selective trafficking into dendritic versus axonal parts of forebrain neurons. However, precise observations of GAP-43 in spines as well as axons of rodent neostriatum (25) suggest that preferred routes of GAP-43 trafficking may vary in subsets of neostriatal neurons as in the corticofugal axonal distribution of RC3. This issue deserves additional consideration since RC3-5 antiserum now eliminates potentially confounded identifications of GAP-43 and RC3.

RC3 in spines raises the possibility that this protein is a point of convergence of several distinct signal transduction pathways. RC3 is a substrate for PKC and a calmodulin-binding protein. The α-subunit of calmodulin kinase II and RC3 have the same cellular distributions. Calmodulin kinase II is associated with postsynaptic densities of asymmetrical axospinous junctions (28, 29). RC3 and calmodulin kinase II interactions, perhaps mediated by calmodulin, could occur in spines of neostriatal neurons. These interactions remain to be elucidated.

In more practical terms, RC3 is a molecular marker that may reflect postsynaptic aspects of formation and remodeling in corticostriatal connections. RC3 levels are likely to diminish in human neurological disorders such as Huntington's disease (30) and AIDS-related dementia (31), which are characterized by neostriatal spine loss. RC3-1 and RC3-5 antisera could be applied usefully to neuropathologic analyses of these diseases because PKC phosphorylation/calmodulin-binding domains of forebrain-enriched RC3 homologs are highly conserved in mammalian evolution (1–3). It is also reasonable to expect the future discovery of comparable PKC phosphorylation/calmodulin-binding domains in proteins associated with dendritic spines of malleable hindbrain cells such as the Purkinje neurons of cerebellar cortex.

Technical assistance was provided by K. Wong (Western blots) and J. Asai (morphology). Research was supported by National Institutes of Health Grants HD25831 (J.B.W.), NS22111 (J.G.S.), and NS24596 (R.S.F.).

1. Watson, J. B., Battenberg, E. F., Wong, K. K., Bloom, F. E. & Sutcliffe, J. G. (1990) *J. Neurosci. Res.* **26,** 397–408.
2. Baudier, J., Deloulme, J. C., Van Dorsselaer, A., Black, D. & Matthes, H. W. D. (1991) *J. Biol. Chem.* **266,** 229–237.
3. Coggins, P. J., Stanisz, J., Nagy, A. & Zwiers, H. (1991) *Neurosci. Res. Commun.* **8,** 49–56.
4. Baudier, J., Bronner, C., Klingman, D. & Cole, R. D. (1989) *J. Biol. Chem.* **264,** 1824–1828.
5. Apel, E. D., Byford, M. F., Au, D., Walsh, K. A. & Storm, D. R. (1990) *Biochemistry* **29,** 2330–2335.
6. Coggins, P. J. & Zwiers, H. (1989) *J. Neurochem.* **53,** 1895–1901.
7. Alexander, K. A., Watkins, B. T., Doyle, G. S., Walsh, K. A. & Storm, D. R. (1988) *J. Biol. Chem.* **263,** 7544–7549.
8. Coggins, P. J. & Zwiers, H. (1990) *J. Neurochem.* **54,** 274–277.
9. Skene, P. J. H. (1989) *Annu. Rev. Neurosci.* **12,** 127–156.
10. Benowitz, L., Apostolides, P., Perrone-Bizzozero, N., Finkelstein, S. & Zwiers, H. (1988) *J. Neurosci.* **8,** 339–352.
11. Represa, A., Deloulme, J. C., Sensenbrenner, M., Ben-Ari, Y. & Baudier, J. (1990) *J. Neurosci.* **10,** 3782–3792.
12. Sutcliffe, J. G., Milner, R. J., Shinnick, T. M. & Bloom, F. E. (1983) *Cell* **33,** 671–682.
13. Wotjtkowiak, Z., Briggs, R. C. & Hnilica, L. S. (1983) *Anal. Biochem.* **129,** 486.
14. Fisher, R. S., Buchwald, N. A., Hull, C. D. & Levine, M. S. (1988) *J. Comp. Neurol.* **272,** 489–502.
15. Jensen, K. F., Ohmstede, C.-A., Fisher, R. S. & Sayhoun, N. (1991) *Proc. Natl. Acad. Sci. USA* **88,** 2850–2853.
16. Powers, M. & Clark, G. (1955) *Stain Technol.* **30,** 83–92.
17. Gabbott, P. L. A. & Somogyi, P. (1984) *J. Neurosci. Methods* **11,** 221–230.
18. Fairen, A., Peters, A. & Saldanha, J. (1977) *J. Neurocytol.* **6,** 311–337.
19. Dray, A. (1980) *Neurobiology* **14,** 221–336.
20. DiFiglia, M., Pasik, T. & Pasik, P. (1980) *J. Neurocytol.* **9,** 471–492.
21. Peters, A., Palay, S. L. & Webster, H. (1991) *The Fine Structure of the Nervous System* (Oxford, New York).
22. Morreale de Escobar, G., Escobar del Rey, F. & Ruiz-Marcos, A. (1983) in *Congenital Hypothyroidism*, eds. Dussault, J. H. & Walker, P. (Decker, New York), pp. 85–126.
23. Munoz, A., Rodriguez-Pena, A., Perez-Castillo, A., Ferreiro, B., Sutcliffe, J. G. & Bernal, J. (1991) *Mol. Endocrinol.* **5,** 273–280.
24. Houbre, D., Duportail, G., Deloulme, J.-G. & Baudier, J. (1991) *J. Biol. Chem.* **266,** 7121–7131.
25. DiFiglia, M., Roberts, R. C. & Benowitz, L. I. (1990) *J. Comp. Neurol.* **302,** 992–1001.
26. Akers, R. F., Lovinger, D. M., Colley, P. A., Linden, R. F. & Routtenberg, A. (1986) *Science* **231,** 587–589.
27. Lovinger, D. M., Colley, P. A., Akers, R. F., Nelson, R. B. & Routtenberg, A. (1986) *Brain Res.* **399,** 205–211.
28. Kennedy, M., Bennett, M. & Erondu, N. (1983) *Proc. Natl. Acad. Sci. USA* **80,** 7357–7361.
29. Burgin, K., Waxham, M., Rickling, S., Westgate, S., Mobley, W. & Kelly, P. (1990) *J. Neurosci.* **10,** 1788–1798.
30. DiFiglia, M. (1990) *Trends Neurosci.* **13,** 286–289.
31. Fisher, R., DeRosa, M. & Vinters, H. (1992) *J. Neuropathol. Exp. Neurol.*, in press.